A unified description of spectra of different configurations, deformation and energy regions

G. Riczu and J. Cseh

Institute for Nuclear Research

Debrecen, Bem ter 18/C, Hungary-4026

Abstract

The multiconfigurational dynamical symmetry (MUSY) is applied for the unified description of the spectra of ^{20}Ne, ^{28}Si, ^{36}Ar, and ^{44}Ti nuclei. They contain shell-like configurations in the ground-state region, core-plus-alpha states above the alpha-separation energy, and exotic cluster states from heavy-ion reactions. The excitation energy and the quadrupole deformation cover large ranges. The gross features of the spectra are reasonably well reproduced by a simple Hamiltonian, in some cases even parameter-free predictions are obtained for high-lying cluster spectra from the low-lying quartet bands in good agreement with experimental observation.

Keywords: Multiconfigurational dynamical symmetry, spectra of different configurations, large energy and deformation regions.

1 Introduction

Our knowledge on nuclear spectrum is clusterized along the energy axis. The most experimental details are available in the ground-state region, of course. With increasing energy the spectrum is less well-established. Above the separation energy of the nucleons or alpha particles a rich set of data is obtained again from the corresponding reactions. Due to the heavy-ion resonances a further region is available at even higher energy. These islands may or may not overlap with each other, and can span as much as 50 MeV, or so.

The physical nature of the states can be very different. In the low-energy region they are usually known to be single-particle or collective excitations, while above the thresholds they can be e.g. core-plus-alpha, or more exotic (^{12}C, ^{16}O,...) cluster states.

From the viewpoint of the deformation the situation is somewhat similar. The well-studied ground-state region usually has a moderate deformation. With

increasing deformation the band structure is less known. When, however, the elongation is large enough, and the ratio of the major axes is near 2:1:1, i.e. we reach the superdeformed shape, then again nice collective bands are seen from multiple coincidence experiments. This region is also called as a second minimum, referring to the next valley of the potential energy. Theoretical studies show a third minimum as well, corresponding to the hyperdeformed shape (3:1:1), and experimental efforts are in line to observe them.

The unified theoretical understanding of these phenomena is a great challenge. Various models are applied for the description of the spectra, usually addressing some definite section of the problem. Comprehensive discussion of different configurations in different ranges of energy and deformation is hardly available. Here we investigate the question, how the multiconfigurational dynamical symmetry (MUSY) is able to account for the gross features of the spectrum in a unified way, incorporating different configurations in a large range of energy and deformation. MUSY is the common intersection of the shell, collective and cluster models for the multi-major-shell problem [1,2].

In what follows first we recall (in Section 2) some basic features of MUSY, then we apply it to four nuclei (in Section 3), each having spectra of different configurations in a large range of excitation energy and quadrupole deformation. Finally (in Section 4) a brief summary is given and some conclusions are drawn.

2   Multiconfigurational dynamical symmetry

MUSY provides us with a unified classification scheme of the shell, collective and cluster models [1,2]. It is defined by the algebra-chain

$$U_s(3) \otimes \; U_e(3) \; \supset U(3) \supset \; SU(3) \supset SO(3). \tag{1}$$

In addition to having a simple dynamical symmetry in each configuration, a further symmetry connects the different configurations to each other [1, 2]. The transformations of the connecting symmetry act in the pseudo space of the particle numbers.

A particularly simple Hamiltonian which is invariant with respect to the connecting transformations is obtained, when it is written in terms of the Casimir operators of the algebras U(3) $\supset$ SU(3) $\supset$ SO(3). An example is presented in detail in the next section.

MUSY bridges the shell and cluster models, as mentioned before. The shell side of MUSY [3], applies a model space which is practically identical with that of the symmetry-adapted no-core shell model (SA-NCSM) [4], apart from the technical difference in the coupling scheme (proton-neutron versus spin-isospin). Therefore, the relation of these two models are very simple. Due to the dynamically symmetric Hamiltonian the shell model in the MUSY is a simplification of the SA-NCSM. But it is not a contraction in the sense how e.g. the contracted symplectic model [5] is obtained from the symplectic model [6].

No bosonization, or any other simplification of the model space is taking place, just the interactions have a (much) simpler form. (In some applications, like here, a simplified version of the shell model is applied, which is called semimicroscopic algebraic quartet model (SAQM) [3], containing only Wigner-scalar $U^{ST}(4)$ representations [7]. This is, however, only a truncation governed by the physical problem, not a model assumption.)

As for the relation to the symplectic [6], and contracted symplectic model [5], the following can be said. By exploring the role of the many major-shell excitations in the shell model description of the collective phenomena these models (together with the cluster model) made possible to find the connecting symmetry (MUSY). In particular in each of these approaches the $U_s(3) \otimes U_e(3) \supset U(3)$ basis gives the classification scheme. This algebraic structure is, however, not connected exclusively to the symplectic algebra (see e.g. [8,9]). In MUSY U(3) bases are applied (not symplectic one).

Due to the microscopic treatment of the model spaces, i.e. all the nucleon degrees of freedom are taken into account, and the Pauli-principle is appreciated, the different configurations may overlap with each other. An especially interesting case is when this overlap is 100%. Such situations can easily be realized once we construct the full no-core shell model space up to a certain excitation number. The shell model basis is complete, therefore, any state vector can be expanded in this basis, and the basis states belonging to different SU(3) irreducible representations (irreps) are orthogonal to each other. Thus in case the multiplicity of the shell model basis of a specific SU(3) irrep is 1, then all the (different cluster) configurations are identical with it, having only a single term in the shell-model expansion. I.e. antisymmetrization may wash out the difference between various configurations.

We stress here, that this consideration is valid only for the basis states, i.e. for the situation when one applies a dynamically symmetric Hamiltonian, in which case the U(3) basis states are energy eigenstates. In reality the configuration mixing is essential, of course, and the real nuclear states are linear combinations of U(3) basis states. To the extent, however, U(3) is a good symmetry the relations we discussed are valid. And several independent studies show that U(3) is a relatively good approximation to many states in the ground-state region, or in shape isomers. Therefore, the overlap mentioned here can play an important role. It is worth emphasising, especially in light of the fact that this aspect is completely neglected in many phenomenological approaches to clusterization, and the shell and different cluster configurations are considered to be orthogonal.

A further interesting feature of the MUSY is that it shows a dual breaking of symmetries. In this respect it is similar to the dynamical symmetry of the Elliott model as well as to many other dynamical symmetries of the nuclear structure models. [10]. In particular, the U(3) and SU(3) symmetries are dynamically broken by the symmetry breaking interaction, represented by the invariant operator of the SO(3) algebra. On the other hand the total Hamiltonian separates into an intrinsic (U(3) and SU(3) dependent), and a collective (SO(3) dependent)

parts. In other words, the fast and slow degrees of freedom are separated. Both parts of the Hamiltonian are SO(3) invariant, but the ground state (and many other states) of the intrinsic Hamiltonian are not rotationally invariant. Thus the SO(3) symmetry is spontaneously broken in the eigenvalue problem of the intrinsic Hamiltonian [11]. Furthermore, as pointed out in the previous paragraph, the nonspherical shape of the intrinsic state can have seemingly different configurations, but the differences might be washed out by the antisymmetrization. When the total Hamiltonian is considered, then the (rotational) symmetry is recovered, as it is usual in the spontaneous breaking [11].

3   Description of spectra by MUSY

Here we show the application of the MUSY for the description of the spectra of ^{20}Ne, ^{28}Si, ^{36}Ar and ^{44}Ti. First we present the way of calculation, then we consider the nuclei one-by-one.

We have applied a simple MUSY Hamiltonian, which has an analytical solution in the U(3)⊃SU(3)⊃SO(3) basis:

$$\hat{H} = (\hbar\omega)\hat{n} + a\hat{C}^{(2)}_{SU(3)} + b\hat{C}^{(3)}_{SU(3)} + d\frac{1}{2\theta}\hat{L}^2, \tag{2}$$

The first term is the harmonic oscillator Hamiltonian (linear invariant of the U(3)), with $\hbar\omega$ oscillator strength. The second order invariant of the SU(3) $\hat{C}^{(2)}_{SU(3)}$ represents the quadrupole-quadrupole interaction, while the third order Casimir-operator $\hat{C}^{(3)}_{SU(3)}$ distinguishes between the prolate and oblate shapes. θ is the moment of inertia calculated classically for the rigid shape determined by the U(3) quantum numbers (for a rotor with axial symmetry) [12]. The $\hbar\omega$, a, b and d parameters were fitted to the experimental data (Table 1). $\hbar\omega$, a, and b are measured in MeV, while d is dimensionless.

	^{20}Ne	^{28}Si	^{36}Ar	^{44}Ti
$\hbar\omega$	6.82481	6.00604	4.88295	5.14846
a	-0.11953	-0.08404	-0.04370	-0.03822
b	-0.00025	0.00061	0.00027	0.00074
d	0.79053	1.33197	1.02914	0.86885
α^2	1.153	0.366	0.466	0.361

Table 1: The parameters of the Hamiltonian and the E2 transitions obtained from a fitting procedure.

The in-band B(E2) value is given as

$$
\begin{aligned}
B(E2, L_i \to L_f) \quad &= \\
&= \frac{2L_f + 1}{2L_i + 1}\alpha^2 |\langle \quad (\lambda\mu) \quad KL_i, (11)2||(\lambda\mu)KL_f\rangle|^2 C^2_{SU(3)}.
\end{aligned}
\tag{3}
$$

where $\langle(\lambda\mu)KL_i,(11)2||(\lambda\mu)KL_f\rangle$ is a SU(3) $\supset$ SO(3) Wigner coefficient [13], and α^2 (measured in W.u.) is a parameter (Table 1).

Now, let's look at the resulting spectra compared to the experiments.

^{20}Ne: This nucleus has a rich experimental spectrum [14,15], which includes also highly-excited alpha-cluster states. The experimentally identified bands are described by the lowest-lying model bands with the appropriate spin-parity content, i.e. the other model bands of the same character are all higher-lying. The 0_1^+, 0^-, 0_4^+, 0_5^+, and 0_6^+ bands are known to have core-plus-alpha character. In the fitting procedure all bands had a unit weight (Figure 1).
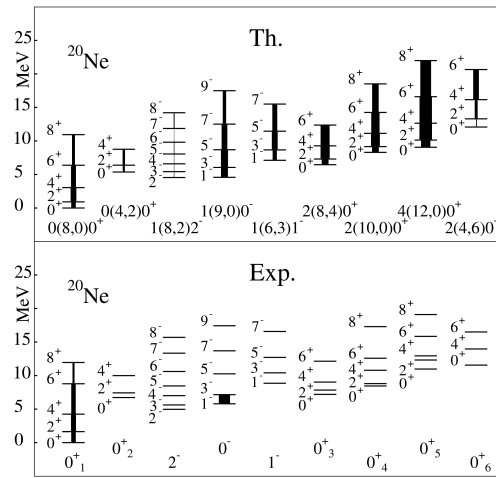

Figure 1: The spectrum of the MUSY (upper part) in comparison with the experimental data of the ^{20}Ne nucleus (lower part). The experimental bands are labeled by the K^π, and the model states by the $n(\lambda,\mu)K^\pi$ quantum numbers. The width of the arrow between the states is proportional to the strength of the E2 transition.

^{28}Si: It has a well-established band-structure in the low-energy region, and to several bands SU(3) quantum numbers could be associated as a joint conclusion of experimental and theoretical investigations [16]. In addition, more recently a new candidate was proposed for the superdeformed (SD) band [17], which is in line with the predictions of theoretical studies [18,19]. Finally, there are two cluster configurations: ^{24}Mg+^{4}He and ^{16}O+^{12}C, belonging to reaction channels in which fine-resolution measurements revealed a rich spectrum of resonances. In the fitting procedure all the low energy bands had a unit weight, the resonances had weight of 0 (Figure 2).

^{36}Ar: This is a special nucleus, because the GS and SD bands of the ^{36}Ar are known experimentally. [20–23] Furthermore, there is a promising candidate
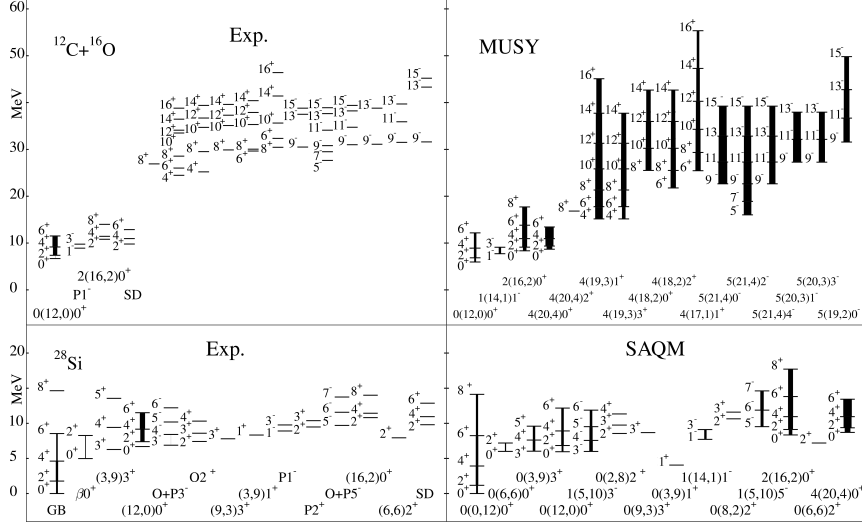
Figure 2: The spectrum of the MUSY in comparison with the experimental data of the ^{28}Si nucleus. The experimental bands are labeled by the available quantum numbers and the other notations are the same as figure 1. The parameters have been fitted to the low-energy part (lower-panel), and the cluster spectrum (upper panel) is obtained as a pure prediction, due to the unified multiplet-stucture and identical physical operators.

for the HD band [24–27]. Besides, in the low-lying region [20–22] we arranged some states into bands according to their energy-differences. In addition, these states are observed as different configurations: shell, ^{32}S+^{4}He, ^{24}Mg+^{12}C, and ^{20}Ne+^{16}O. The U(3) quantum numbers of the GS, SD and HD states were determined from a symmetry stability and self-consistency calculation [27]. The other HD band (of negative parity) are associated with the band that was closest to the positive band in deformation and had appropriate spin-parity content. Finally, we assigned the most deformed representations of 0 and 1 $\hbar\omega$ model space to the three low-energy bands, that had appropriate spin-parity content. In the fitting procedure the better-known GS and SD bands had a unit weight, the other bands had weight of 0.01 (Figure 3).

We determined the shapes of some of the states as well (Figure 4). From the shell model side the quadrupole shape is given by the U(3) quantum numbers. The ^{20}Ne+^{16}O, ^{24}Mg+^{12}C, ^{32}S+^{4}He cluster configurations can be obtained from the Harvey prescription [28, 29] and from the U(3) selection rule [30–32] which describes the structural aspect of the fusion (or fission) of a nucleus in terms of the harmonic oscillator basis. Since the multiplicity of the relevant U(3) representation is 1 in the shell basis, these shell and cluster con-

figurations turn out to be identical with each other, due to the effect of the anti-symmetrization (Figure 4).
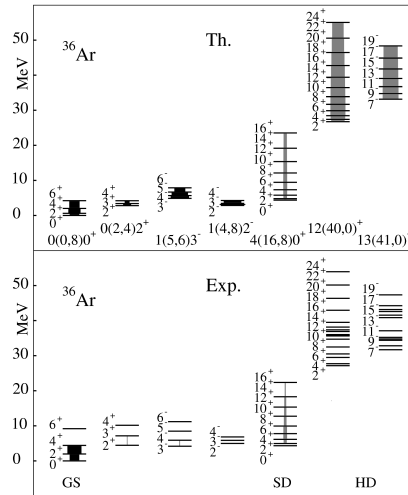

Figure 3: The spectrum of the MUSY in comparison with the experimental data of the ^{36}Ar nucleus. The notations are the same as Figure 1. The real strength of the gray arrows (of the SD and HD bands) are 20 times of the illustrated ones.

^{44}Ti: This nucleus has some well-established low-lying bands [33], and in addition a reliable experimental evidence is available for core-plus-alpha states forming four bands [34]. Furthermore, high-lying resonances are populated in the ^{28}Si+^{16}O reactions [35]. The low-lying bands [33] are associated to those of the leading SU(3) representations of the quartet model, which correspond to the largest deformation. The alpha-cluster bands correspond to the lowest-lying Pauli-allowed representations. Concerning the ^{28}Si+^{16}O cluster states, we associate their positive and negative parity bands with the leading representations of the 4 and 5 $\hbar\omega$ excitations. Around this excitation a shape isomer of the ^{44}Ti nucleus is expected according to the calculations [36] of the self-consistency and stability of the (quasidynamical) SU(3) symmetry (which is uniquely related to the quadrupole deformation) In the fitting procedure the well-known states of the low-lying bands had a unit weight, the states with uncertain spin parity (in parentheses in compilation [33]) had weight of 0.5 (Figure 5).
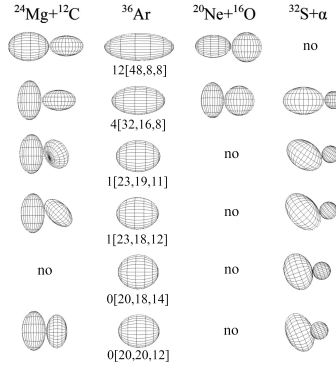
Figure 4: Shape of some states in ^{36}Ar in increasing energy order. In [ ] parenthesis, the U(3) labels are indicated, while the first integer shows the major shell excitation quanta. Note, that the multiplicity of these U(3) states in the shell basis is 1, therefore, the indicated shell, and cluster configurations have wavefunctions with 100% overlap in each case, as a consequence of the antisymmetrization.
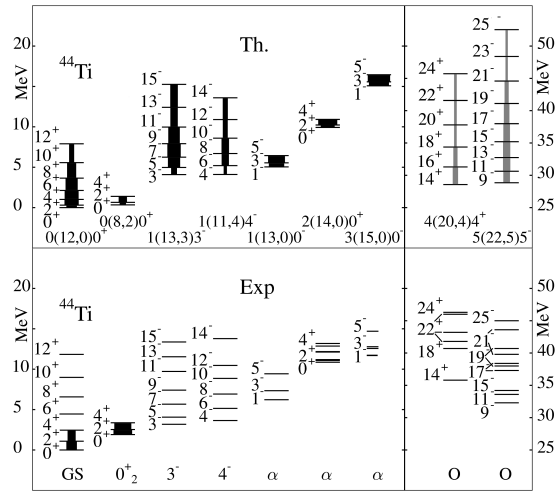

Figure 5: The spectrum of the MUSY in comparison with the experimental data of the ^{44}Ti nucleus. In the experimental spectrum α indicates the alpha-cluster states, while O means the ^{28}Si+^{16}O resonances. The other notations are the same as Figure 1. The real strength of the gray arrows (^{16}O bands) is five times the strength of the illustrated ones.

4 Summary and conclusions

In this paper we have applied the multiconfigurational dynamical symmetry for the description of spectra of a large range of excitation energy and deformation, and having various physical nature. We have considered self-conjugate ($N = Z$) nuclei, and described their low-lying spectra with the semimicroscopic quartet model [3], while highly excited states were treated as alpha or more exotic cluster states. MUSY is able to give a unified spectra due to the fact that it is the common intersection of the shell, collective and cluster models for the multi-major-shell problem. In particular, it has an $U_s(3) \otimes U_e(3)$ dynamical symmetry in each configuration, and furthermore, another symmetry (in the particle-index space) connects the different configurations to each other.

The Hamiltonians which are invariant with respect to the transformations from one configuration to another are expressed in terms of operators that are contracted in the particle index [1, 2]. A particularly simple form is when H is obtained in terms of invariant operators, but even this condition allows a great variety, and in our previous applications [1,3,37,38] we have tried some of them. Here we used a single functional form for the calculation of the spectra of four nuclei: ^{20}Ne, ^{28}Si, ^{36}Ar, ^{44}Ti. It has four terms, each with well-defined physical meaning: oscillator quantum, quadrupole interaction, deformation energy (prolate or oblate), moment of inertia.

It turns out that a simple Hamiltonian with analytical solution is able to account for the gross features of the spectra of light nuclei in a wide range of energy (sometimes up to 50 MeV), and deformation (normal, super- and hyper-deformation) for states of different configurations (shell, collective, and various clusters). In case of ^{28}Si (where a rich and well-established band structure is known) we could even extrapolate for the high-lying cluster spectra (^{16}O+^{12}C, ^{24}Mg+^{4}He) from of the low-lying quartet spectrum. It is especially remarkable that this parameter-free prediction is in good agreement with the experimental observation.

In addition to giving a unified description of the spectra MUSY also reveals the interrelations of different configurations. A particularly interesting feature is the total overlap of the wave functions of the shell and (different) cluster models. An illustrative example for the ^{36}Ar nucleus is presented in Figure 4.

The approach we presented here shows a considerable similarity to the symmetry-adapted no-core shell model [4, 39, 40]. The model space of both frameworks are microscopic and no-core, i.e. incorporates all nucleons. (The difference in the coupling scheme: proton-neutron in the SA-NCSM, and spin-isospin in the MUSY is only a technical one, and they can be transformed into each other [41].)

The SA-NCSM applies both model interactions and real nucleon-nucleon forces, in the latter case it is a real ab initio method. The symmetry (SU(3) and symplectic) as well as the collective and cluster states emerge from a first-principle calculation. With MUSY we take a complementary approach, by addressing the question, how a simple dynamically symmetric Hamiltonian is able

to describe the shell (or quartet), collective and cluster states in a unified framework. These states are defined by shell (or quartet), collective and cluster models, which have a common multiplet structure within the MUSY.

In short: MUSY is a model symmetry (in the intersection of semimicroscopic models), which can not compete, of course, with real microscopic and ab initio calculation, like SA-NCSM. This latter one reveals the existence of symplectic and SU(3) as emergent symmetries from a first principle calculation. (It is worth noting, however, that the shape isomers are given by the emerging U(3) symmetry also in case of MUSY. In particular the stable and selfconsistent SU(3) symmetry is obtained from a model-calculation with symmetry-breaking terms [36].)

Due to the close similarities (comparable or identical model spaces, governing role of U(3) symmetry), however, MUSY seems to be a useful possibility for the extension of the SA-NCSM to ranges of more exotic clusterizations, and to extreme deformations etc, i.e. into the regions, which are beyond the limits of the present day calculations for the fully microscopic treatment.

Acknowledgements

References

[1] J. Cseh (2021) *Phys. Rev.* C **103** 064322.

[2] J. Cseh (2021) *Bulg. J. Phys.* **8** 457.

[3] J. Cseh (2015) *Phys. Lett. B.* **743** 213.

[4] T. Dytrych, K.D. Sviratcheva, J.P. Draayer, C. Bahri, and J.P. Vary (2008) *J. Phys.* G **35** 123101.

[5] D. J. Rowe, G. Rosensteel (1982) *Phys. Rev.* C **25** 3236(R);
     O. Castanos, J. P. Draayer (1989) *Nucl. Phys.* A **491** 349

[6] G. Rosensteel, D. J. Rowe (1977) *Phys. Rev. Lett.* C **38** 10;
     (1980) *Ann. Phys. (N.Y.)* **126** 343;
     D. J. Rowe (1985) *Rep. Prog. Phys.* **48** 1419

[7] E. P. Wigner (1937) *Phys. Rev.* **51** 106.

[8] D. J. Rowe, G. Thiamova, J. L. Wood (2006) *Phys. Rev. Lett.* **97** 202501.

[9] G. Thiamova, D. J. Rowe, J. L. Wood (2006) *Nucl. Phys. A.* **780** 112.

[10] J. Cseh (2020) *Eur. Phys. J. A Spec. Top.* **229** 2543.

[11] J. Cseh (2019) *Phys. Lett.* B **793** 59.

[12] J. Cseh (2015) *J. Phys. Conf. Ser.* **580** 012046.

[13] Y. Akiyama and J.P. Draayer (1973) *Comput. Phys. Commun.* **5** 405.

[14] D.R. Tilley et al. (1998) *Nucl Phys.* A **636** 249.

[15] H.T. Richards (1984) *Phys. Rev. C* **29** 276.

[16] R.K. Sheline et al. (1982) *Phys. Lett.* B **119** 263.

[17] D.G. Jenkins et al. (2012) *Phys. Rev. C* **86** 064308.

[18] Y. Taniguchi, Y. Kanada-En'yo, M. Kimura (2009) *Phys. Rev.* C **80** 044316.

[19] J. Darai, J. Cseh, D.G. Jenkins (2012) *Phys. Rev. C* **86** 064309.

[20] N. Nica, J. Cameron and B. Singh (2012) *Nuclear Data Sheets* **113** 1.

[21] https://www.nndc.bnl.gov/nudat2/getdatasetClassic.jsp?nucleus=36AR&unc=nds

[22] https://www-nds.iaea.org/relnsd/vcharthtml/VChartHTML.html

[23] C.E. Svensson et al. (2001) *Nucl. Phys.* A **682** 1.

[24] W.D.M. Rae and A.C. Merchant (1992) *Phys. Lett.* B **279** 207.

[25] J. Cseh, A. Algora, J. Darai and P.O. Hess (2004) *Phys. Rev. C* **70** 034311.

[26] W. Sciani et al. (2009) *Phys.Rev.* C **80** 034319.

[27] J. Cseh et al. (2009) *Phys. Rev.* C **80** 034320.

[28] M. Harvey (1975) *Proc. 2nd Int. Conf. on Clustering Phenomena in Nuclei* (College Park,USDERA report ORO-4856-26), p. 549.

[29] J. Cseh and J. Darai (2008) *AIP Conf. Proc.* **1098**: Fusion08 p. 225.

[30] B.F. Bayman and A. Bohr (1958/59) *Nucl. Phys.* **9** 596.

[31] J. Cseh and W. Scheid (1992) *J. Phys.* G **18** 1419.

[32] J. Cseh (1993) *J. Phys.* G **19** L97.

[33] https://www.nndc.bnl.gov/ensdf/EnsdfDispatcherServlet.

[34] S. Ohkubo et al. (1998) *Prog. Theor. Phys. Suppl.* **132** 1 and references therein; T. Yamaya, S. Oh-ami, M. Fujiwara, T. Itahashi, K. Katori, M. Tosaki, S. Kato, S. Hatori, and S. Ohkubo (1990) *Phys. Rev.* C **42** 1935; P. Guazzoni et al. (1993) *Nucl. Phys.* A **564** 425.

[35] U. Abbondanno (1991) Trieste Report No. INFN/BE-91/11

[36] J. Cseh, G. Riczu and J. Darai (2019) *Phys. Lett.* B **795** 160.

[37] J. Cseh and G. Riczu (2016) *Phys. Lett.* B **757** 312.

[38] G. Riczu, J. Cseh (2021) *Int. J. Mod. Phys.* E **30** 2150034.

[39] J.P. Draayer, contribution to the present workshop

[40] T. Dytrych, contribution to the present workshop

[41] J. Cseh, G. Riczu, J. Darai, T. Dytrych and E. Betak (2017) *Bulg. J. Phys.* **44** 466.